



Title	A copper nitride nanocube catalyst for highly efficient hydroboration of alkynes
Author(s)	Xu, Hang; Yamaguchi, Sho; Mitsudome, Takato et al.
Citation	Organic and Biomolecular Chemistry. 2023, 7, p. 1404-1410
Version Type	AM
URL	https://hdl.handle.net/11094/90056
rights	Reproduced from Org. Biomol. Chem., 2023, 7, 1404-1410 with permission from the Royal Society of Chemistry.
Note	

The University of Osaka Institutional Knowledge Archive : OUKA

<https://ir.library.osaka-u.ac.jp/>

The University of Osaka

ARTICLE

Copper nitride nanocube catalyst for the highly efficient hydroboration of alkynes

Hang Xu,^a Sho Yamaguchi,^a Takato Mitsudome^{a,b} and Tomoo Mizugaki^{*a,c}Received 00th January 20xx,
Accepted 00th January 20xx

DOI: 10.1039/x0xx00000x

Hydroboration of alkynes with bis(pinacolato)diboron is a useful method for the synthesis of vinyl boronate esters, which are essential intermediates in organic syntheses. Copper catalysts have been used extensively in these reactions. However, previously reported Cu-catalyst systems inevitably require additives and elevated temperatures. Herein, we report, for the first time, the simple and efficient hydroboration of alkynes under additive-free and mild reaction conditions (i.e., at a temperature of 30 °C) using a copper nitride nanocube (Cu₃N NC) catalyst. A wide range of alkynes can be transformed into their corresponding boronate esters. Cu₃N NCs are also applicable in the hydroboration of alkynes with tetrahydroxydiboron to synthesize vinyl boronic acids. Moreover, Cu₃N NCs were easily separated by simple filtration and could be reused several times without any loss to their original activity. Hence, these highly active and reusable Cu₃N NC catalysts offer an environment-friendly route for the efficient production of vinyl boronates.

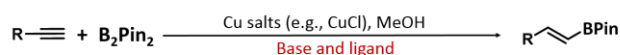
Introduction

Vinyl boronate esters are important and versatile building blocks in pharmaceutical chemistry¹ and synthetic organic chemistry². They serve as key nucleophilic reagents in cross-coupling reactions for C–N, C–O, and C–C bond formation.³ The hydroboration of alkynes with pinacolborane (HBPin) is a useful method for the synthesis of vinyl boronate esters.⁴ However, HBPin is difficult to handle due to its moisture and oxygen sensitivity.⁵ As a result, the catalytic hydroboration of alkynes with water-resistant and oxygen-insensitive bis(pinacolato)diboron (B₂Pin₂) has attracted significant attention.⁶ To date, there have been many reports of homogeneous Cu catalytic systems, but the catalysts in these systems are difficult to separate and recycle (Scheme 1A).⁷ To overcome these drawbacks, some efforts have been devoted to developing heterogeneous Cu catalysts, such as CuO/MgO, Cu metal–organic frameworks (Cu-MOF), and Cu nanospheres/graphene nanosheets (Cu-NPs/rGO) (Scheme 1B).⁸ However, these catalytic systems require the use of additives to activate the B₂Pin₂. Recently, remarkable research has been reported by Li's group using single-atom Cu catalysts for the hydroboration of alkynes under additive-free conditions.⁹ Despite their high catalytic performance, thermal

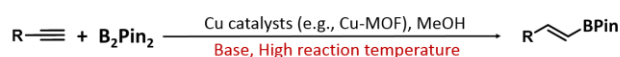
conditions are still needed. Consequently, an efficient and environmentally benign catalytic system for the selective hydroboration of alkynes under mild and additive-free conditions remains in great demand.

Nano-sized particles of metal non-oxide compounds, such as metal nitrides, phosphides, and sulfides, are a new class of catalytic materials in organic syntheses.¹⁰ Recently, we reported on the high catalytic activity of copper nitride (Cu₃N) in liquid-phase reactions.¹¹ Cu₃N possesses a regularly arranged N–Cu–N structure on the surface, and the interaction between adjacent Cu and N atoms creates the unique catalysis of Cu₃N. In this work, we report that the Cu₃N nanocubes (Cu₃N NCs) act as a highly active heterogeneous catalyst for the hydroboration of various alkynes with diborons in ethanol (EtOH) to the corresponding vinyl boronate esters (Scheme 1C). This is the first example of heterogeneous Cu catalysts for the hydroboration of alkynes under additive-free and mild reaction conditions.

A) Homogeneous Cu catalytic systems:



B) Heterogeneous Cu catalytic systems:



C) This work:

Scheme 1 Copper-catalyzed hydroboration of terminal alkynes with B₂Pin₂.

^a Department of Materials Engineering Science, Graduate School of Engineering Science, Osaka University, 1-3 Machikaneyama, Toyonaka, Osaka 560-8531, Japan

E-mail: mizugaki.tomoo.es@osaka-u.ac.jp

^b PRESTO, Japan Science and Technology Agency (JST), 4-1-8 Honcho, Kawaguchi, Saitama 333-0012, Japan

^c Innovative Catalysis Science Division, Institute for Open and Transdisciplinary Research Initiatives (ICS-OTRI), Osaka University, Suita, Osaka 565-0871, Japan

† Footnotes relating to the title and/or authors should appear here.

Electronic Supplementary Information (ESI) available: [details of any supplementary information available should be included here]. See DOI: 10.1039/x0xx00000x

Experimental

General information

All organic reagents were purchased from FUJIFILM Wako Pure Chemical Corporation, Sigma–Aldrich, or Tokyo Chemical Industry. Gas chromatography-mass spectrometry (GC-MS) was performed using a GCMS-QP2010 SE instrument equipped with an InertCap WAX-HT capillary column (GL Science, 30 m × 0.25 mm i.d., film thickness 0.25 μm). ^1H and ^{13}C nuclear magnetic resonance (NMR) spectra were acquired at 400 and 100 MHz, respectively, using a JEOL JNM-ESC400 spectrometer. All known compounds described in this paper were characterized by comparing their ^1H and ^{13}C NMR spectra with previously reported data. Scanning electron microscopy (SEM) images were obtained using a JSM-7600F microscope operated at 15.0 kV at the Analytical Instrument Facility, Graduate School of Science, Osaka University. Transmission electron microscopy (TEM) images were obtained using a Hitachi HF-2000 microscope operated at 200 kV at the Research Center for Ultra-High-Voltage Electron Microscopy, Osaka University. Cu K -edge X-ray absorption spectra (extended X-ray absorption near edge structure (XANES)) obtained using a Si(111) monochromator were recorded at 25 °C at the BL01B1 and BL14B2 stations at SPring-8, Japan Synchrotron Radiation Research Institute (JASRI), Harima, Japan, and the data analysis was performed using Demeter (ver. 0.9.26) software. Powder X-ray diffraction (PXRD) patterns were acquired using a Philips XPert-MPD instrument with Cu- K_α radiation. X-ray photoelectron spectroscopy (XPS) spectra of the samples were obtained using a KRATOS AXIS ULTRA HAS spectrometer, and the binding energy was referenced to the C 1s peak (284.4 eV). Fourier-transform infrared (FT-IR) spectra were recorded on a JASCO FT-IR 4100 spectrometer equipped with a mercury cadmium telluride detector. FT-IR attenuated total reflectance (ATR) spectra were recorded on a SHIMADZU IRSprite-T spectrometer. Temperature-programmed desorption (TPD) data were obtained using a BELCAT-A instrument (BEL Japan Inc.) equipped with a mass spectrometer (BELMass-S, BEL Japan, Inc.).

Preparation of Cu_3N NCs

Cu_3N NCs were synthesized based on our previous work.^{11b} Briefly, $\text{Cu}(\text{NO}_3)_2 \cdot 3\text{H}_2\text{O}$, octadecylamine, and oleylamine were added to a Schlenk flask. The mixture was then heated to 260 °C under an Ar atmosphere to yield a brown colloidal solution. After cooling to room temperature, the solid was isolated via precipitation in 2-propanol. The obtained solid was washed several times with EtOH/toluene (v/v = 1/1) to afford Cu_3N NC as a brown powder.

Procedure for catalytic hydroboration of alkynes

The general procedure for the hydroboration of alkynes using Cu_3N NCs is as follows. The Cu_3N NC catalyst (5 mg) was placed in a 50-mL stainless-steel autoclave with a Teflon inner cylinder, with alkynes (0.5 mmol), diboron reagents (0.6 mmol), and EtOH (2 mL). The mixture was stirred at 30 °C under an Ar atmosphere. After the reaction, the solution was analyzed by GC-MS or ^1H NMR spectroscopy to determine the

regioselectivity. The mixture was concentrated to yield the crude product, which was further purified using silica gel flash chromatography (hexane/ethyl acetate) to give the desired products.

Gram-scale experiment

Cu_3N NCs (2 mg, 0.01 mmol of Cu) were placed in a 50-mL stainless-steel autoclave with a Teflon inner cylinder, with phenylacetylene (**1a**) (1.02 g, 10.0 mmol), B_2Pin_2 (3.03 g, 12.0 mmol), and EtOH (10 mL). The reaction mixture was stirred at 30 °C under an Ar atmosphere for 12 h. After the reaction, the reaction mixture was concentrated to yield the crude product, which was further purified using silica gel flash chromatography (hexane/ethyl acetate, v/v = 30/1) to give (*E*)-4,4,5,5-tetramethyl-2-styryl-1,3,2-dioxaborolane (**2a**) (2.09 g).

Results and discussion

Characterization of Cu_3N NCs

The formation of the pristine Cu_3N NCs was confirmed by PXRD analysis (Fig. 1a). The five diffraction peaks at $2\theta = 23.1^\circ$, 33.2° , 40.9° , 47.6° , and 53.7° correspond to the standard diffraction data for copper nitride (JCPDS No. 47-1088).¹² Cu K -edge XAFS analysis was performed to investigate the oxidation state of the Cu species in the Cu_3N NCs. Figure 1b shows the XANES spectrum of the Cu_3N NCs along with the spectra of Cu foil, CuO , and Cu_2O as references. The absorption edge energy of the Cu_3N NCs was similar to that of Cu_2O , indicating that the Cu species in the Cu_3N NCs is in the +1 oxidation state. Furthermore, the representative SEM and TEM images revealed the cubic structure of the Cu_3N NCs with an average edge length of 67 nm (Figs. 1c, 1d, and S1).

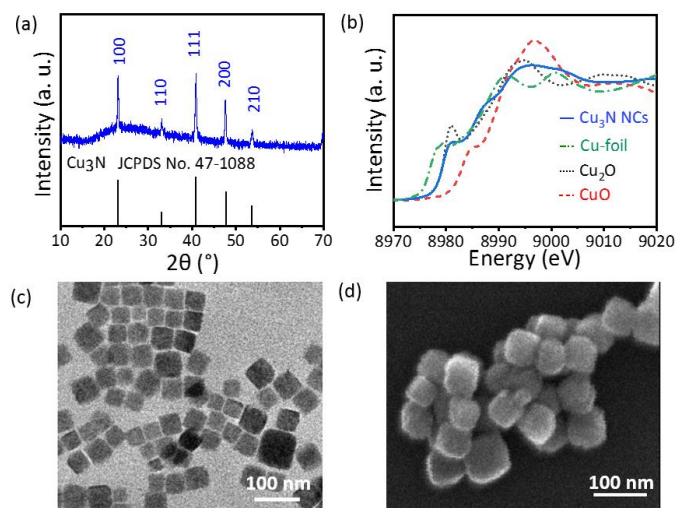
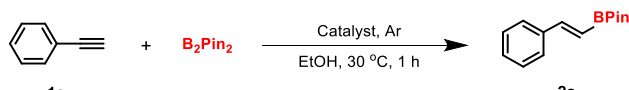


Fig. 1 (a) PXRD patterns of Cu_3N NCs. (b) Cu K -edge XANES spectra of Cu_3N NCs and the reference Cu compounds. (c) TEM and (d) SEM images of Cu_3N NCs.

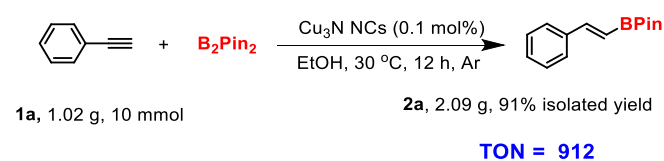
Catalytic performance evaluation

The catalytic activity of the Cu_3N NCs was examined for the hydroboration of **1a** with B_2Pin_2 in EtOH. Notably, the Cu_3N NC catalyst showed high activity for the hydroboration of **1a**,

Table 1 Hydroboration of **1a** using various Cu catalysts.^a

		
Entry	Catalyst	Yield of 2a (%) ^b
1	Cu ₃ N NCs	99
2	Cu ₂ O	<1
3	CuO	<1
4	Cu ₂ O NCs	<1

^a Reaction conditions: **1a** (0.5 mmol), catalyst (5 mol% of Cu), and EtOH (2 mL) under Ar. ^b Yield was determined by ¹H NMR analysis using 1,4-dinitrobenzene (0.1 mmol) as an internal standard.

**Scheme 2** A gram-scale experiment of the hydroboration of **1a** to **2a** using Cu₃N NCs.

providing **2a** in quantitative yield without base additives (Table 1, Entry 1, for details, see Table S1). This is the first example of a heterogeneous Cu catalyst that promotes the hydroboration of **1a** with B₂Pin₂ under additive-free conditions at 30 °C (Table S2). In contrast to the excellent catalytic performance of Cu₃N NCs, the mono- and divalent Cu reference catalysts, Cu₂O and CuO respectively, were almost inactive under the same reaction conditions (Table 1, Entries 2 and 3). Furthermore, Cu₂O NCs with the same morphology and size as the Cu₃N NCs were prepared (For details, see Fig. S2)¹³ and used in the hydroboration of **1a**, but no product (**2a**) was obtained (Table 1, Entry 4). The Cu₃N NC catalyst system was also applicable in gram-scale synthesis, affording **2a** in 91% isolated yield with a turnover number (TON) of 912, based on the total number of Cu atoms used in the reaction (Scheme 2). These results clearly demonstrate the high catalytic activity of Cu₃N NCs in the hydroboration of **1a**.

The Cu₃N NC catalyst was easily recovered by centrifugation and was reused in multiple experiments. The recovered Cu₃N NC catalyst exhibited no obvious loss in activity after the third recycling experiment (Fig. 2a). To investigate the heterogeneous nature of the Cu₃N NCs during the reaction, a hot filtration experiment was performed (Fig. 2b). No additional product was formed in the filtrate after the Cu₃N NC catalyst was removed by filtration, indicating that hydroboration of **1a** proceeded on the Cu₃N NC surface. The reused Cu₃N NCs were analyzed by PXRD, TEM, and XAFS. The PXRD patterns of the recovered Cu₃N NCs displayed the same five peaks as those of the fresh Cu₃N NCs (Fig. S3). The TEM image confirmed that there were no significant changes in the shape and size of the recovered Cu₃N NCs (Fig. S4). In addition, the XANES analysis showed that the absorption edge energy of the reused Cu₃N NCs was similar to that of the fresh catalyst (Fig. S5). These results confirm the high durability of the Cu₃N NC catalyst under the utilized hydroboration conditions.

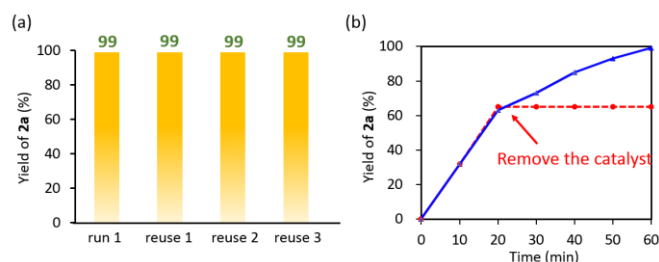
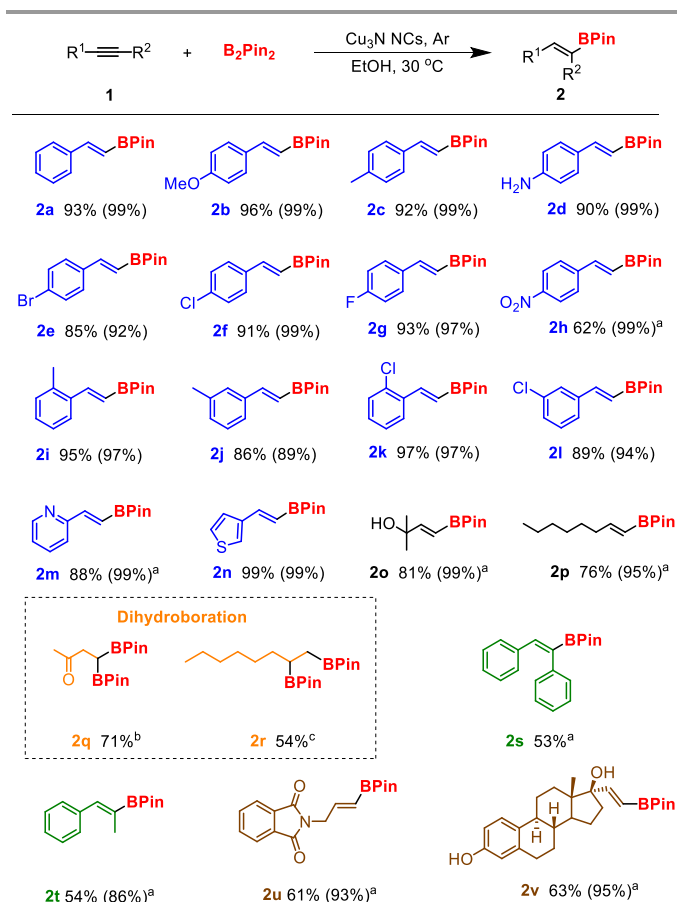


Fig. 2 (a) Reuse experiments of Cu₃N NCs in the hydroboration of **1a** to **2a** for 1 h. (b) Hot filtration experiment of Cu₃N NCs in the hydroboration of **1a** to **2a**: without catalyst removal (blue line) and with catalyst removal (red dot line). Reaction conditions: Cu₃N NCs (5 mg), **1a** (0.5 mmol), B₂Pin₂ (0.6 mmol), EtOH (2 mL), 30 °C, Ar. Yields were calculated by ¹H NMR analysis using 1,4-nitrobenzene as an internal standard.

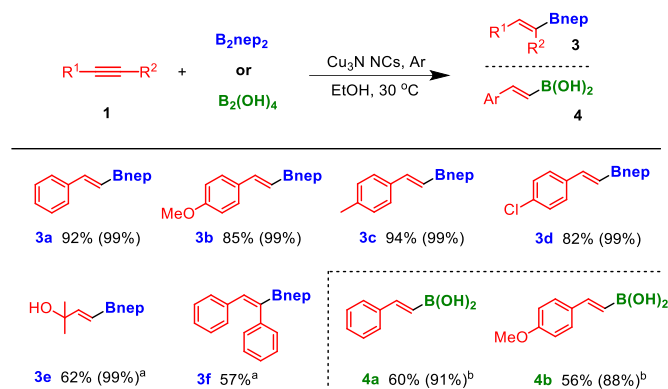
The substrate scope was then explored (Scheme 3). Various 1-ethynylbenzenes bearing electron-donating groups (–OMe, –Me, and –NH₂) and electron-withdrawing groups (–Br, –Cl, –F, and –NO₂) at the para-position were successfully converted to the corresponding borylated products in 62–96% isolated yields with excellent regio- and stereoselectivity (**2b–2h**). Ortho- and meta-substituted 1-ethynylbenzenes were also borylated,



Scheme 3 Hydroboration of various alkynes with B₂Pin₂. Reaction conditions: **1** (0.5 mmol), B₂Pin₂ (0.6 mmol), Cu₃N NCs (5 mg, 5 mol% of Cu), EtOH (2 mL), Ar, 30 °C, 1 h. Isolated yields. Regioselectivity in parentheses was determined by GC-MS or ¹H NMR analysis. ^a 12 h. ^b **1q** (0.2 mmol), B₂Pin₂ (0.5 mmol), Cu₃N NCs (2 mg, 5 mol% of Cu), EtOH (1 mL), 80 °C, 1 h. ^c **1r** (0.25 mmol), B₂Pin₂ (1.0 mmol), Cu₃N NCs (5 mg, 10 mol% of Cu), EtOH (1 mL), 80 °C, 12 h, yield was determined by ¹H NMR analysis using 1,4-dinitrobenzene (0.1 mmol) as an internal standard.

affording the desired vinyl boronic esters in 86–97% yields (**2i**–**2l**). Heteroaromatic alkynes, 2-ethynylpyridine and 3-ethylthiophene, underwent hydroboration to give the corresponding products in 88% and 99% yields, respectively (**2m** and **2n**). In addition, aliphatic terminal alkynes were efficiently converted to the desired boronate esters in 81% and 76% yields, respectively (**2o** and **2p**). Moreover, the Cu_3N NC catalytic system was applied to the dihydroboration of alkynes for synthesizing diborylalkanes, which are essential intermediates for organic transformations.¹⁴ A conjugated ynone, but-3-yn-2-one (**1q**), with 2.5 eq. of B_2Pin_2 afforded the geminal diboryl product (**2q**) in 71% yield.^{8f} While in the reaction of 1-octyne with 4 eq. of B_2Pin_2 , 1,2-diborylated octane (**2r**) was the major product obtained in 54% yield.¹⁵ Phenylacetylene resulted in the poor regioselectivity; the mixture of geminal and 1,2-addition products were obtained, which may be caused by the protodeborylation of the intermediates (see Scheme S1 for the details of limitation of substrate).^{15b,16} This is the first example of a heterogeneous metal catalyst for the dihydroboration of alkynes with B_2Pin_2 under additive-free conditions.^{8f,17} The hydroboration of internal alkynes afforded the corresponding products in moderate yields (**2r** and **2s**). Bioactive phthalimide and steroid derivatives were also tolerated, and afforded **2t** and **2u** in 61% and 63% isolated yields, respectively. These results demonstrate the high functional group tolerance and utility of Cu_3N NCs for fine chemical syntheses.

Hydroboration of alkynes with other diboronate reagents was subsequently investigated (Scheme 4). Bis(neopentylglycolato)diboron (B_2nep_2) reacted efficiently with various aromatic alkynes to generate the corresponding vinyl boronate esters in 82–94% yields (**3a**–**3d**). Aliphatic alkyne, 2-methylbut-3-yn-2-ol, and internal alkyne, 1,2-diphenylethyne, were favorable for this reaction, and the desired products were obtained in 62% and 57% yields, respectively (**3e** and **3f**).



Scheme 4 Hydroboration of various alkynes with B_2nep_2 or $\text{B}_2(\text{OH})_4$. Reaction conditions: **1** (0.5 mmol), B_2nep_2 or $\text{B}_2(\text{OH})_4$ (0.6 mmol), Cu_3N NCs (5 mg, 5 mol% of Cu), EtOH (2 mL), Ar, 30 °C, 1 h. Isolated yields. Regioselectivity in parentheses was determined by ^1H NMR analysis. ^a 12 h. ^b 3 h.

Subsequently, we investigated the hydroboration of alkynes with $\text{B}_2(\text{OH})_4$ to synthesize vinyl boronic acids, which are useful in pharmaceutical and organic chemistry.¹⁸ A previously reported system required multiple steps,¹⁹ while the present Cu_3N NC catalyst efficiently promoted the direct hydroboration of several terminal aryl alkynes to the corresponding vinyl boronic acids in good yields (**4a** and **4b**).

Reaction mechanism

To gain insight into the origin of the high catalytic activity of Cu_3N NCs, various spectroscopic analyses of Cu_3N NCs and Cu_2O NCs were performed. The FT-IR spectrum of the Cu_3N NCs after pyridine absorption displayed three peaks at 1594, 1576, and 1442 cm^{-1} , attributed to the coordination of pyridine to Lewis acid sites (Fig. 3a, blue line).²⁰ Furthermore, CO_2 -TPD measurements clearly revealed the presence of base sites on the Cu_3N NC surface (Fig. 3b, blue line). In sharp contrast to the

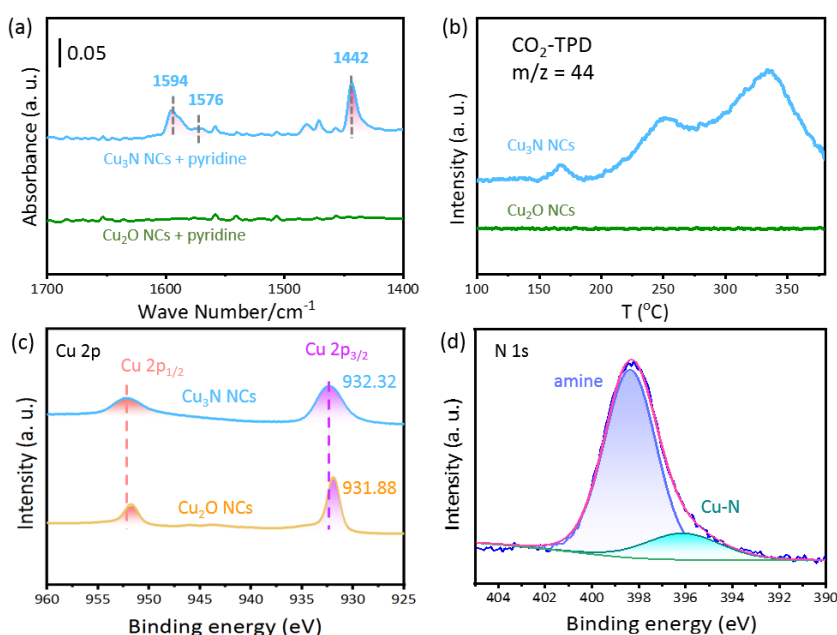


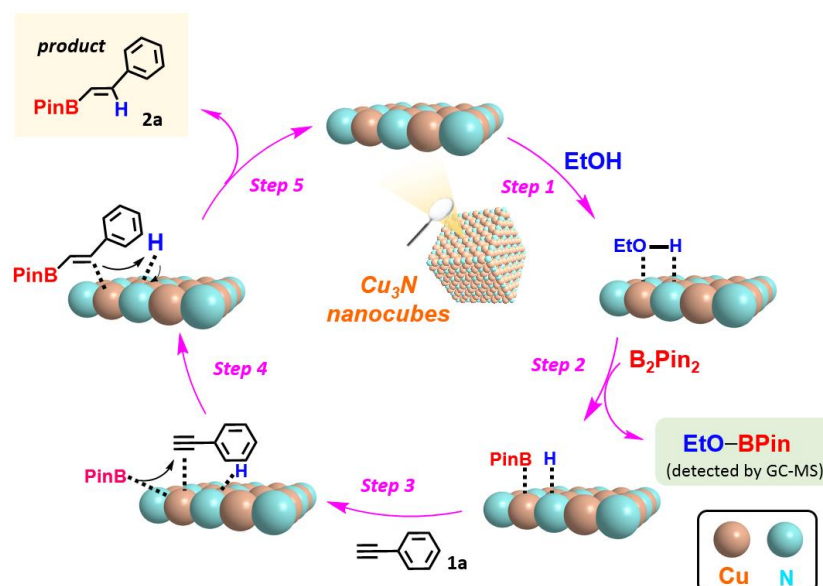
Fig. 3 (a) FT-IR spectra of pyridine absorbed on Cu_3N NCs (blue line) and Cu_2O NCs (green line). (b) CO_2 -TPD signals of Cu_3N NCs (blue line) and Cu_2O NCs (green line) monitored at $m/z = 44$. (c) Cu 2p XPS spectra of Cu_3N NCs and Cu_2O NCs. (d) N 1s XPS spectrum of Cu_3N NCs.

Cu₃N NCs, there are no absorption peaks in the FT-IR and CO₂-TPD spectra of the Cu₂O NCs (Figs. 3a and 3b, green line) (for details, see Fig. S6 and Table S3). We further performed XPS analysis of the Cu₃N NCs. The Cu 2p_{3/2} peak in the Cu₃N NC spectrum was observed at 932.3 eV which is slightly higher than that for the Cu₂O NCs (Fig. 3c).²¹ This observation is due to the electron transfer from Cu to N atoms in Cu₃N NCs and the resulting Cu Lewis acid sites on Cu₃N NCs.²² Furthermore, the N 1s peak of Cu₃N NC displayed two contributions: from the Cu–N (396.2 eV) species and the residual surface amines (398.3 eV) (Fig. 3d).^{23,24} Therefore, the excellent catalytic performance of Cu₃N NCs may be attributed to the co-existence of Lewis acid-base sites.²⁵

Based on the co-existence of Lewis acid and base sites on Cu₃N NCs, a reaction mechanism is proposed in Scheme 5.^{7,8} First, EtOH is adsorbed and activated on the surface of sites of Cu₃N NCs (step 1). Then, the activated EtOH reacts with B₂Pin₂ to form a Cu–BPin species, along with the production of EtO–BPin (step 2). Subsequently, nucleophilic attack of the Cu–BPin

species on **1a**, activated by the Lewis acid site of Cu, forms a linear intermediate (steps 3 and 4).^{9b,26} Finally, a hydrogen transfer process occurs to provide the desired product **2a** (step 5).

The above reaction pathway was supported by the following experimental results. 1) EtO–BPin was detected by GC-MS (Fig. S7). 2) When borylation of **1a** was performed in monodeuterized ethanol (EtOD), monodeuterized **2a** (**2a-d**) was obtained as the main product (see Scheme S2a and Figs. S8 and S9). To consider the rate-determining step in this reaction, we also estimated the kinetic isotope effect (KIE) in the reaction of **1a** in EtOH or EtOD solvent (Scheme S2b): the KIE value was 3.2, which is similar with the KIE value listed in reported works,^{25,27} suggesting that the abstraction of O–H bond of alcohol would be the rate determining step. Thus, the distinct catalytic activity of Cu₃N NCs can be attributed to the cooperative catalysis of Lewis acid-base sites for the sequential activation of EtOH, B₂Pin₂, and the alkyne.^{25,28}



Scheme 5 Proposed mechanism of the hydroboration of **1a** catalyzed by Cu₃N NCs.

Conclusions

Herein we have reported the highly efficient hydroboration of alkynes over a Cu₃N NC catalyst under additive-free and mild reaction conditions. The utility of the Cu₃N NC catalyst was demonstrated for the reaction of a wide variety of alkynes with diboron compounds, including B₂(OH)₄, affording the corresponding vinyl boronate esters and vinyl boronic acids in good-to-excellent yields. The Cu₃N NCs exhibited high catalytic performance even at 30 °C and were applicable to gram-scale production with an excellent TON (912). The heterogeneous Cu₃N NC catalyst was easily separated and reused at least three times with excellent yields. The co-existence of Lewis acid-base sites on the Cu₃N NC surface plays a key role in accelerating the

hydroboration of alkynes. We believe that copper nitride has great potential as a replacement for conventional Cu catalysts and makes a significant contribution to the development of green and sustainable reaction processes.

Author Contributions

H. X. designed the experiments, conducted catalytic activity tests, and characterized the catalysts. S. Y. and T. Mit. discussed the experiments and the results. T. Miz. directed and conceived the project. H. X. and S. Y. co-wrote the manuscript with input from all authors. All authors commented on the manuscript and approved its final version.

Conflicts of interest

There are no conflicts to declare.

Acknowledgements

This work was supported by JSPS KAKENHI Grant Numbers 20H02523 and 21K04776 and JST PRESTO Grant Number JPMJPR21Q9. This study was partially supported by JST-CREST Grant Number JPMJCR21L5. Part of the experimental analysis was supported by the “Nanotechnology Platform” Program at Hokkaido University (A-21-HK-0051) and the Nanotechnology Open Facilities in Osaka University (A-20-OS-0025) of MEXT. We thank Dr. Toshiaki Ina and Dr. Tetsuo Honma (SPring-8) for the XAFS measurements (2021B1176, 2021B1898, and 2022A1772).

Notes and references

- 1 J. W. B. Fyfe and A. J. B. Watson, *Chem*, 2017, **3**, 31–55.
- 2 K. Yang and Q. Song, *Acc. Chem. Res.*, 2021, **54**, 2298–2312.
- 3 N. Miyaura and A. Suzuki, *Chem. Rev.*, 1995, **95**, 2457–2483.
- 4 For selected reviews: (a) K. Kuciński and G. Hreczycho, *Green Chem.*, 2020, **22**, 5210–5224; (b) S. Rej, A. Das and T. K. Panda, *Adv. Synth. Catal.*, 2021, **363**, 4818–4840; (c) Y. Mutoh, K. Yamamoto, Y. Mohara and S. Saito, *Chem. Rec.*, 2021, **21**, 1–14; (d) J. Hu, M. Ferger, Z. Shi and T. B. Marder, *Chem. Soc. Rev.*, 2021, **50**, 13129–13188; (e) J. Walkowiak, J. Szyling, A. Franczyk and R. L. Melen, *Chem. Soc. Rev.*, 2022, **51**, 869–994.
- 5 J. F. Li, Z. Z. Wei, Y. Q. Wang and M. Ye, *Green Chem.*, 2017, **19**, 4498–4502.
- 6 For selected reviews: (a) T. Ishiyama and N. Miyaura, *Chem. Rec.*, 2004, **3**, 271–280; (b) J. Yun, *Asian J. Org. Chem.*, 2013, **2**, 1016–1025; (c) S. K. Bose, L. Mao, L. Kuehn, U. Radius, J. Nekvinda, W. L. Santos, A. W. Stephen, G. S. Patrick and T. B. Marder, *Chem. Rev.*, 2021, **121**, 13238–13341.
- 7 (a) J. E. Lee, J. Kwon and J. Yun, *Chem. Commun.*, 2008, 733–734; (b) G. Stavber and Z. Časar, *Appl. Organometal. Chem.*, 2013, **27**, 159–165; (c) H. Yoshida, Y. Takemoto and K. Takaki, *Chem. Commun.*, 2014, **50**, 8299–8302; (c) Y. E. Kim, D. Li and J. Yun, *Dalton Trans.*, 2015, **44**, 12091–12093; (d) Q. Feng, K. Yang and Q. Song, *Chem. Commun.*, 2015, **51**, 15394–15397; (e) A. K. Nelson, C. L. Peck, S. M. Rafferty and W. L. Santos, *J. Org. Chem.*, 2016, **81**, 4269–4279.
- 8 (a) A. Grirrane, A. Corma and H. Garcia, *Chem. Eur. J.*, 2011, **17**, 2467–2478; (b) J. Zhao, Z. Niu, H. Fu and Y. Li, *Chem. Commun.*, 2014, **50**, 2058–2060; (c) L. Xu and B. Xu, *Tetrahedron Lett.*, 2017, **58**, 2542–2546; (c) X. Zeng, C. Gong, H. Guo, H. Xu, J. Zhang and J. Xie, *New J. Chem.*, 2018, **42**, 17346–17350; (d) C. Zhang, M. Zhou, S. Liu, B. Wang, Z. Mao, H. Xu, Y. Zhong, L. Zhang, B. Xu and X. Sui, *Carbohydr. Polym.*, 2018, **191**, 17–24; (e) H. Y. Tsai, M. Madasu and M. H. Huang, *Chem. Eur. J.*, 2019, **25**, 1300–1303; (f) Z. L. Wu, X. Lan, N. Gao, X. Kang, Z. Wang, T. Hu and B. Zhao, *J. Catal.*, 2021, **404**, 250–257; (g) L. J. Zhang, J. C. Yuan, L. J. Ma, Z. Y. Tang and X. M. Zhang, *J. Catal.*, 2021, **401**, 63–69; (h) B. Wang, L. Gao, H. Yang and G. Zheng, *ACS Appl. Mater. Interfaces*, 2021, **13**, 47530–47540; (i) R. J. Wei, P. Y. You, H. Duan, M. Xie, R. Q. Xia, X. Chen, X. Zhao and G.-H. Ning, *J. Am. Chem. Soc.*, 2022, **144**, 17487–17495.
- 9 (a) J. Zhang, Z. Wang, W. Chen, Y. Xiong, W. C. Cheong, L. Zheng, W. Yan, L. Gu, C. Chen, Q. Peng, P. Hu, D. Wang and Y. Li, *Chem*, 2020, **6**, 725–737; (b) W. H. Li, J. Yang, H. Jing, J. Zhang, Y. Wang, J. Li, J. Zhao, D. Wang and Y. Li, *J. Am. Chem. Soc.*, 2021, **143**, 15453–15461.
- 10 For selected reviews: (a) S. Carenco, D. Portehault, C. Boissiere, N. Mezailles and C. Sanchez, *Chem. Rev.*, 2013, **113**, 7981–8065; (b) Q. Gao, N. Liu, S. Wang and Y. Tang, *Nanoscale*, 2014, **6**, 14106–14120; (c) H. Hao and X. Lang, *ChemCatChem*, 2019, **11**, 1378–1393; (d) D. R. Aireddy and K. Ding, *ACS Catal.*, 2022, **12**, 4707–4723; our recent works: (e) S. Fujita, K. Nakajima, J. Yamasaki, T. Mizugaki, K. Jitsukawa and T. Mitsudome, *ACS Catal.*, 2020, **10**, 4261–4267; (f) S. Yamaguchi, S. Fujita, K. Nakajima, S. Yamazoe, J. Yamasaki, T. Mizugaki and T. Mitsudome, *Green Chem.*, 2021, **23**, 2010–2016; (g) H. Ishikawa, S. Yamaguchi, A. Nakata, K. Nakajima, S. Yamazoe, J. Yamasaki, T. Mizugaki and T. Mitsudome, *JACS Au*, 2022, **2**, 419–427.
- 11 (a) H. Xu, S. Yamaguchi, T. Mitsudome and T. Mizugaki, *Org. Biomol. Chem.*, 2021, **19**, 6593–6597; (b) H. Xu, S. Yamaguchi, T. Mitsudome and T. Mizugaki, *Eur. J. Org. Chem.*, 2022, e202200826.
- 12 R. Deshmukh, G. Zeng, E. Tervoort, M. Staniuk, D. Wood and M. Niederberger, *Chem. Mater.*, 2015, **24**, 8282–8288.
- 13 A. M. Elseman, M. S. Selim, L. Luo, C. Y. Xu, G. Wang, Y. Jiang, D. B. Liu, L. P. Liao, Z. Hao and Q. L. Song, *ChemSusChem*, 2019, **12**, 3808–3816.
- 14 K. Endo, M. Hirokami and T. Shibata, *J. Org. Chem.*, 2010, **75**, 3469–3472.
- 15 (a) Y. Lee, H. Jang and A. H. Hoveyda, *J. Am. Chem. Soc.*, 2009, **131**, 18234–18235; (b) G. Gao, J. Yan, K. Yang, F. Chen and Q. Song, *Green Chem.*, 2017, **19**, 3997–4001.
- 16 (a) G. Gao, Z. Kuang and Q. Song, *Org. Chem. Front.*, 2018, **5**, 2249–2253; (b) S. Rao and K. R. Prabhu, *Chem. Eur. J.*, 2018, **24**, 13954–13962.
- 17 (a) M. Gao, S. B. Thorpe and W. L. Santos, *Org. Lett.*, 2009, **11**, 3478–3481; (b) Y. Netsu and N. Tsukada, *Lett. Org. Chem.*, 2017, **14**, 243–247.
- 18 (a) J. M. Stevens and D. W. MacMillan, *J. Am. Chem. Soc.*, 2013, **135**, 11756–11759; (b) D. G. Hall, *Chem. Soc. Rev.*, 2019, **48**, 3475–3496.
- 19 (a) A. V. Kalinin, S. Scherer and V. Snieckus, *Angew. Chem. Int. Ed.*, 2003, **42**, 3399–3404; (b) Y. Ma, B. R. P. Reddy and X. Bi, *Org. Lett.*, 2019, **21**, 9860–9863.
- 20 V. S. Escribano, C. del Hoyo Martínez, E. F. López, J. G. Amores and G. Busca, *Catal. Commun.*, 2009, **10**, 861–864.
- 21 Z. Yin, C. Yu, Z. Zhao, X. Gou, M. Shen, N. Li, M. Muzzio, J. Li, H. Liu, H. Lin, J. Yin, G. Lu, D. Su and S. Sun, *Nano Lett.*, 2019, **19**, 8658–8663.
- 22 X. H. Li and M. Antonietti, *Chem. Soc. Rev.*, 2013, **42**, 6593–6604.
- 23 (a) R. K. Sithole, L. F. E. Machogo, M. A. Airo, S. S. Gqoba, M. J. Moloto, P. Shumbula, J. Van Wyk and N. Moloto, *New J. Chem.*, 2018, **42**, 3042–3049; (b) M. Parvizian, A. D. Balsa, R. Pokratath, C. Kalha, S. Lee, D. Van den Eynden, M. Ibanez, A. Regoutz and J. De Roo, *Angew. Chem. Int. Ed.*, 2022, **134**, e202207013.
- 24 Y.-X. Liu, H.-H. Wang, T.-J. Zhao, B. Zhang, H. Su, Z.-H. Xue, X.-H. Li and J.-S. Chen, *J. Am. Chem. Soc.*, 2019, **141**, 38–41.
- 25 S. Furukawa, M. Ieda and K. Shimizu, *ACS Catal.*, 2019, **9**, 5096–5103.
- 26 P. Zhang, J. Meijide Suárez, T. Driant, E. Dera, Y. Zhang, M. Ménand, S. Roland and M. Sollogoub, *Angew. Chem. Int. Ed.*, 2017, **56**, 10821–10825.
- 27 M. Aelterman, M. Sayes, P. Jubault and T. Poisson, *Chem. Eur. J.*, 2021, **27**, 8277–8282.
- 28 (a) K. Shimizu, K. Kon, K. Shimura and S. S. M. A. Hakim, *J. Catal.*, 2013, **300**, 242–250; (b) G. S. Foo, F. Polo-Garzon, V. Fung, D.-E. Jiang, S. H. Overbury and Z. Wu, *ACS Catal.*, 2017, **7**, 4423–4434.